Korean J. Chem. Eng., **30**(4), 864-870 (2013)
DOI: 10.1007/s11814-012-0205-y

Effect of support for alcohol-hydrocarbon synthesis from syngas in Cu-based catalyst

Sun-Hwa Yeon†, Dae-Hyun Shin, Nam-Sun Nho, Kyoung-Hee Shin, Chang-Soo Jin, and Sung-Chan Nam

Energy Storage Group, Korea Institute of Energy Research, 152, Gajeong-ro, Yuseong-gu, Daejeon 305-343, Korea
(*Received 21 June 2012 • accepted 26 November 2012*)

Abstract−Effects of a Cu-based catalyst on the catalytic performance in alcohol-hydrocarbon synthesis from syngas have been investigated, using various supports. Under the different porosities of three supports (zinc oxide, activation carbon, and titanium dioxide), whereas Cu/ZnO produces one liquid phase of major mixed alcohols, Cu/AC and Cu/TiO_2 create two phases, alcohol (~75%) and hydrocarbon (~25%). X-ray diffraction shows that CuO impregnated on supports undergoes a complete reduction of metallic copper Cu^0, which is the real active phase in the catalytic process. The Cu/TiO_2 catalyst showed the highest ethanol composition in a mixed alcohol phase under GHSV 18,000 h^{-1}, 30 bar, and 300 °C.

Key words: Ethanol, Catalyst, Copper, Zinc Oxide, Activated Carbon, Titanium Dioxide, Support

INTRODUCTION

World energy consumption, which has reached unprecedented levels during the past century, is still highly dependent on natural resources, such as petroleum, natural gas, and coal. Fossil fuels are finite, and their current consumption rate is higher than their corresponding regeneration rate. Therefore, new sources of energy with the potential to effectively replace fossil fuels are required for future generations [1].

The production of renewable fuels such as alcohols, including ethanol in particular, has received considerable attention for use in automobiles, chemical additives, and as a potential source of hydrogen for fuel cells [2,3]. Gasification of biomass to syngas (CO and H_2), followed by catalytic conversion, provides an attractive route to produce ethanol in large ethanol quantities [4]. A substantial amount of research has been performed on the catalytic conversion route for ethanol synthesis. Biomass gasification means incomplete combustion of biomass resulting in production of combustible gases consisting of carbon monoxide (CO), hydrogen (H_2) and traces of methane (CH_4), in which this mixture is called synthesis gas (syngas). Syngas can be used to operate internal combustion engines and to produce an attractive chemical as environmentally-friendly fuels such as methanol and ethanol - an extremely attractive chemical which is useful both as fuel for heat engines as well as chemical feedstock for industries. Usually, the synthesis of ethanol from biomass-derived syngas is essentially based on hydrogenation reactions, i.e., hydrogenation of CO or CO_2 with H_2 or H_2O to C_2^+ products ($2CO+4H_2 \rightarrow C_2H_5OH+H_2O$, $H_2/CO=2.0$). Side reactions involving these compounds such as the water-gas shift ($CO+H_2O \leftrightarrow CO_2+H_2$) and methanation reactions also occur. The water gas shift reaction is a very important reaction that affects the equilibrium of both CO and CO_2 hydrogenation reactions and that provides the H_2 to meet H_2/CO ratio 2.0. In the case of H_2-poor syngas (lower H_2/CO ratios in the feed), the syngas conversion and the CH_4 selectivity decreased, while the C_5^+ selectivity and olefin/paraffin ratio for C_2-C_4 increased slightly with decreasing ethanol production.

The major hurdles for ethanol production from syngas are low yield and poor selectivity when associated with the use of known catalysts [5,6]. One of the great challenges in catalyst research, along with developing a fundamental understanding of catalytic function, is the design of improved catalysts. To make the catalytic conversion route attractive, it is essential to develop more effective catalysts by redesigning them with promoters or supports.

Two groups of well-known catalyst candidates for ethanol production have been developed to date. First, supported Rh-based catalysts are known to preferentially convert syngas to C_2^+ oxygenates relative to C_1 oxygenates [7,8], following the reaction mechanism of CO and CO_2 hydrogenation. This is due to the ability of supported Rh catalyst particles to simultaneously adsorb CO in both molecular and dissociated states [8,9]. In the case of SiO_2-supported Rh catalysts, hydrogenation of CO yields various products including methane and higher hydrocarbons, methanol, ethanol and higher alcohols, acetaldehyde, acetic acid, and other higher oxygenates, depending upon the reaction conditions, supports, and promoters [7,9,10]. Research on the effects of different carbonaceous materials (Carbon Black, CMK, and Activated Carbon) as supports for Rh - based catalysts has been performed for catalyzing syngas conversion to C_2 oxygenates [11]. In multi-component promoted Rh catalysts, a combination of nano channels and a graphitic structure plays an important role in promoting the reaction, in addition to the metal dispersion and particle size. However, due to the high cost of noble metals such as Rh, Rh based catalysts have an economic disadvantage. Therefore, they are usually prepared with a low loading, ranging from 0.5 to 2 wt%.

Second, extensive development of catalysts for ethanol production has been achieved through the study of modified methanol synthesis catalysts, for example, alkali-doped Cu/Zn, Cu/Zn/Al, and Cu/Zn/Cr catalyst systems [12,13]. Metals such as Cu, Zn, and Al are inexpensive and provide excellent performance as a typical catalyst for methanol synthesis. Most of the work reported on modified methanol catalysts for CO hydrogenation to higher alcohols has been

†To whom correspondence should be addressed.
E-mail: ys93@kier.re.kr

on Cu-based catalysts, proposing a chain growth mechanism on modified Cu/Zn catalyst and K/Cu/Zn/Al catalyst [14]. However, regardless of the choice of catalyst or conditions (promoter concentration or H_2/CO ratio), methanol is mainly produced on these catalysts [15]. The catalysts are usually prepared using bimetals or three metals of Cu, Zn, and Al, including diverse supports or oxide forms, due to synergism between the constituents of multi-component catalysts [16]. In the case of multicomponent metal-supported catalysts, however, it is difficult to elucidate the crucial effects of each individual component, for example, between each metal and its support, on the alcohol production.

In this paper, Cu-based catalysts were prepared at 3-5 wt% Cu and their catalytic activity were studied with three different supports, zinc oxide (ZnO), activation carbon (AC), and titanium dioxide (TiO_2), for alcohol-hydrocarbon synthesis from syngas. Within the mixed products of alcohol and hydrocarbon, we focus on the amount and composition of ethanol product. We examine the pore texture of different supports and the structural changes of the supported Cu catalyst after the catalytic reaction.

EXPERIMENTAL SECTION

1. Catalyst Preparation

Supported Cu catalysts were synthesized by incipient wetness impregnation. Copper (II) nitrate trihydrate ($Cu(NO_3)_2 \cdot 3H_2O$, Junsei Chemical Co., Ltd.) was used as the precursor of Cu for all catalysts. Commercial ZnO, activated carbon, and TiO_2 were used as support. A 3-5 wt% Cu/AC catalyst was prepared by dissolving 1.2 g of Copper(II) nitrate trihydrate in 6 mL of distilled deionized water and adding this solution dropwise with proper kneading to 6 g of support to the point of incipient wetness. The paste was dried overnight in air at 100 °C and subsequently calcined under an argon atmosphere at 400 °C for 4 h. Two other catalysts were prepared in a similar manner.

2. Reaction of CO and H_2

The prepared catalysts were evaluated in a fixed-bed channel reactor (I.D.: 8 mm, L: 450 mm) system. In this study, the choice of reactor material is a critical factor for the reaction using a carbon-containing gas such as CO. In the gasification process, stainless steel provides high resistance to corrosion under conditions of high pressure and temperature. However, small metal particles or alloys such as Ni, Fe, or Co from the stainless steel reactor wall start to detach over the condition of 400 °C and 30 bar, due to the H_2 and CO gas stream contact. Therefore, they act as another catalyst during the reaction, affecting the reaction performance. In this study, the conditions for the catalytic reaction are temperature below 300 °C and pressure of 30 bar. The reactor is micro channel reactor, where the gas diffusion effects between catalyst particles can be ignored. Approximately 1.0 cm^3 of catalyst was loaded and packed into the center of the reactor. The top of the catalyst was covered by silica wool, upon which quartz sand was packed to help distribution of the feed gases into the catalyst bed. The catalyst was then reduced under a mixed gas flow (H_2/Ar (10/90 vol%), 20 cm^3 (STP) min^{-1}) at 400 °C for 2 h under atmospheric pressure. Following reduction, the catalysts were tested at nominally identical conditions of 200 °C to 300 °C, 20-30 atm total pressure, syngas flow of 100 to 400 cm^3 (STP) min^{-1}, H_2 : CO ratio of 2 : 1 (feed gas, H_2/CO=63.6/33.3 mol%), and a GHSV of 6,000 to 24,000 $cm^3 \cdot V_{cat}^{-1} \cdot h^{-1}$. Two thermo-couples composed of the same material as the reactor were installed on and under the catalyst bed to monitor and control the temperature. The temperature difference between the top and bottom catalyst bed was controlled within ±2 °C, indicating excellent heat removal capability of the channel reactor. Outflow from the catalytic reactor at 200-300 °C after reaction penetrates the high-pressure container (cylindrical type, Diameter: 5 cm, Length: 10 cm) connected to a chiller set at −10 °C. The condenser can completely liquefy a gas mixture at high temperature, such as alcohol and hydrocarbon, into the cooler container. In 5 h operation at constant pressure, temperature, and feed amount, the liquefied products in the container were weighed and analyzed by GCMASS chromatography.

3. Catalyst Characterization

The pore structures of the prepared materials were verified by the nitrogen sorption isotherm at −196 °C (Belsorp, BEL Japan, Inc.), which is sensitive to pore sizes in a range from 1.5 to 50 nm. The pore size distribution was determined from the adsorption branch of the isotherms using Barrett-Joyner-Halenda (BJH) method, and surface areas were estimated from the nitrogen sorption data using Brunauer-Emmett-Teller (BET) analysis. XRD patterns were collected using step scans, with a step size of 0.01° (2θ) and a count time of 2s per step between 5 (2θ) and 80 (2θ). A gas liquid chromatography mass spectrometry analysis was performed with a Shimadzu QP 5050A mass spectrometer coupled to a Shimadzu 17A gas chromatograph fitted with a split-split less injector and a DB-5 fused-silica capillary column (30 m×0.25 mm i. d., 0.25 umfilm thickness). Helium was used as the carrier gas at a flow rate of 1 ml/min. The injection port was maintained at 250 °C, and the split ratio was 1 : 40. Oven temperature programming was carried out from 50 to 280 °C at 10 °C/min, and the oven was kept at 280 °C for 5 min. The interface temperature was kept at 250 °C. Ionization mode was electron impact ionization and the scanning range was from 40 amu to 400 amu. Mass spectra were obtained at 0.5 sec. The peaks obtained from GC-MASS were assigned from the GC-MS Wiley database (6^{th} edition).

RESULTS AND DISCUSSION

Fig. 1 shows the produced liquid amount of 3 wt% Cu/ZnO as a function of GHSV, pressure, and concentration of Cu on ZnO at 300 °C. All products obtained from the Cu/ZnO catalysts are a single liquid phase of mixed alcohols and hydrocarbons at room temperature. The produced liquid amount is 0.15-0.3 g/h between GHSV 6,000 and 18,000 h^{-1} at 300 °C and 20-30 bar, as shown in Fig. 1(a). The liquid amount increases from 0.2 g/h to 0.3 g/h as the GHSV increases from 6,000 h^{-1} to 18,000 h^{-1} at 20 bar and 300 °C. At 30 bar, the amount at 6,000 h^{-1} increases from 0.18 g/h to 0.2 g/h until 12,000 h^{-1}, then decreases to 0.16 g/h at 18,000 h^{-1}. However, when the pressure is increased from 20 bar to 30 bar, the total liquid amount deceases by 20-50% at all GHSV ranges. Fig. 2 shows the original GC/MASS chromatogram of the produced liquid phase under 5 wt% Cu/ZnO and 3 wt% Cu/ZnO, which is obtained to confirm the components of the produced liquid and the effects of two different metal concentrations. The components at 5 wt% Cu/ZnO are similar to those at 3 wt% Cu/ZnO, consisting of H_2O and various alcohols, such as methanol, ethanol, propanol, butanol, pentanol, hexanol,

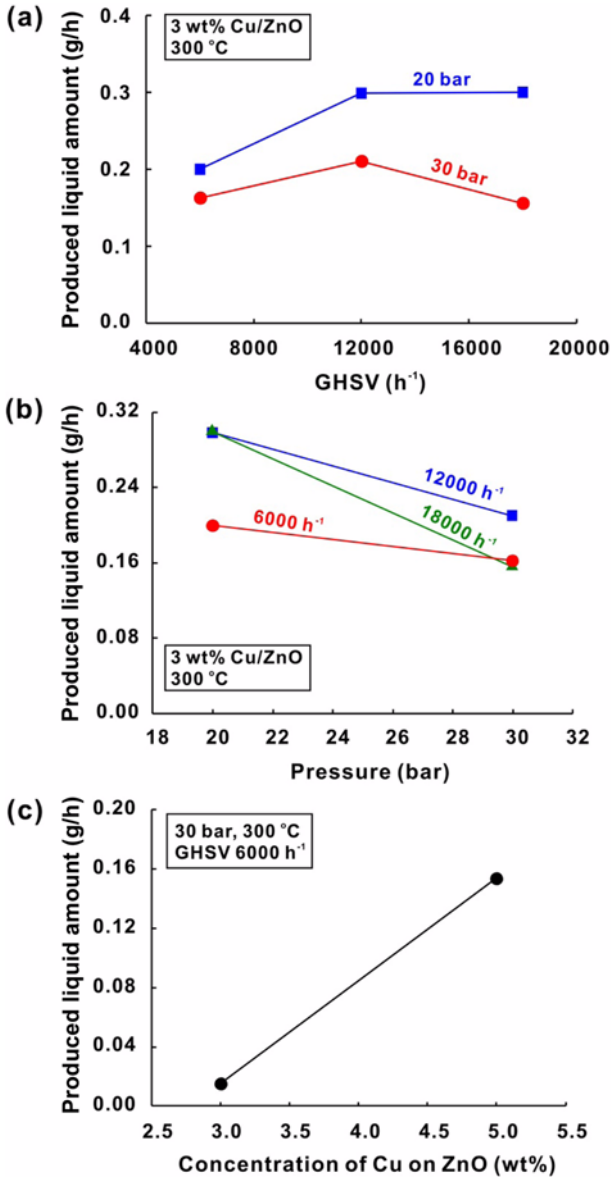

Fig. 1. The produced amount of liquid phase of 3 wt% Cu/ZnO on the variance of GHSV, pressure and concentration of Cu on ZnO.

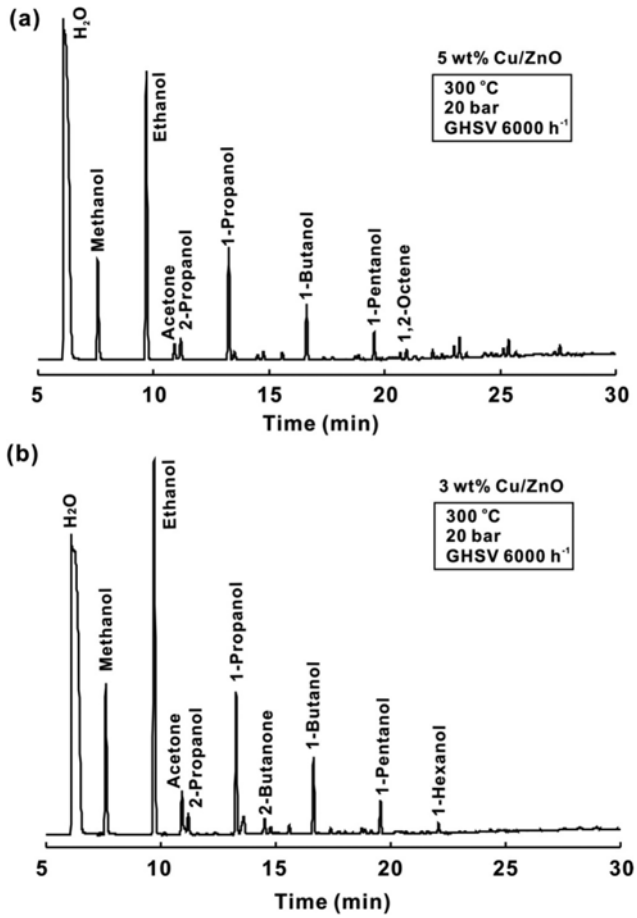

Fig. 2. Original GC/MASS chromatogram of produced liquid phase under (a) 5 wt% Cu/ZnO and (b) 3 wt% Cu/ZnO catalysts.

and so on. However, the compositions of these mixed alcohol and aqueous phase are slightly different. Table S1 shows the components and percent composition of the produced liquid at 5 wt% and 3 wt% Cu/ZnO, respectively. In both 5 wt% and 3 wt% Cu/ZnO, the main phase is the water phase, 57.5% and 55.8%, respectively, and the ethanol portion is largest in the mixed alcohol phases, 15.3% and 18.2%, respectively. Also, at 3 wt% Cu, the portions of methanol, propanol, and butanol are 45%, 12%, and 18%, respectively, which are higher than those at 5 wt% Cu.

To confirm the effects of the support on the catalytic properties of Cu catalysts for the syngas reaction, we used activated carbon and titanium dioxide as supports at 5 wt% Cu metal concentration. Carbon is the most frequently used support due to its high surface area, high porosity, and various textural properties. Figs. 3(a) and (b) show comparisons of adsorption-desorption isotherms for N_2 at −196 °C between AC and 5 wt% Cu/AC and BET specific surface area of the samples before and after Cu loading on supports. All the isotherms belong to two types, type I at low relative pressures (P/P_0) and type IV at intermediate and high relative pressures. The marked hysteresis observed in the nitrogen adsorption confirms the presence of mesoporosity in AC and 5 wt% Cu/AC (Fig. 3(a)). After loading 5 wt% Cu, the BET specific surface area decreases by about 8% with little change in the total pore volume. In this case, while the mesopore volume (estimated from BJH calculation) increases to about 7%, the microprobe volume (estimated from t-plot) decreases to about 30%, as shown in Table S2. This might result from an increase of mesopore volume by carbon loss of the support AC during the calcinations (400 °C) and a decrease of micropores through a blocking effect by the loaded Cu.

To compare the structure of the Cu-supported catalysts, X-ray diffraction (XRD) studies were performed for three catalysts before and after the syngas reaction (Fig. 4). Prior to the syngas reaction, the Cu impregnated on the support became oxide form, CuO, during the calcination process at 400 °C, as shown in Figs. 4 (a)-(c). This CuO is used as a catalyst in chemical reactions that involve hydrogen as a reactant: methanol, ethanol, or hydrocarbon synthesis from CO. In several of these catalytic processes, CuO undergoes a complete reduction and metallic copper or Cu^0 is the real active phase [17-19]. After CuO is exposed to mixtures of Ar/H_2 for a reduction

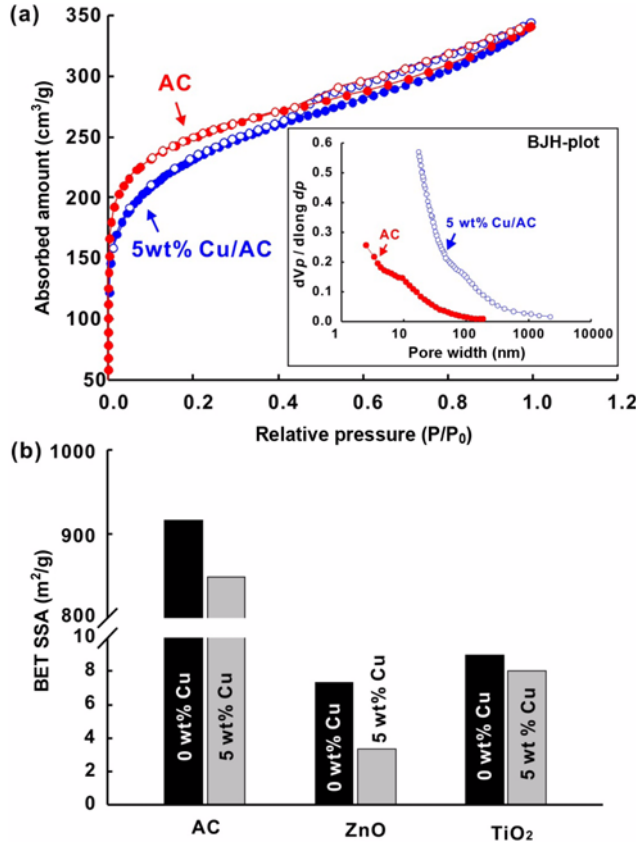

Fig. 3. Comparisons of adsorption-desorption isotherms for N_2 at 77 K between AC and 5 wt% Cu/AC and BET specific surface area (SSA) of the samples before and after Cu loading on AC, ZnO and TiO_2 supports.

process and CO/H_2 for the catalytic reaction, XRD pattern of Figs. 4(a)-(c), clearly show a CuO→Cu transformation at 5 wt% Cu/AC sample after H_2 reduction and the catalytic reaction. Single-crystal surfaces of metallic copper give reaction rates and kinetic parameters that match those obtained for the reaction on CuO/ZnO catalysts, suggesting that an active Cu^0 is produced during the reaction.

Fig. 5 shows the amount of liquid phase produced at 5 wt% Cu/AC and 5 wt% Cu/TiO_2, respectively, under 30 bar and 300 °C. All products obtained from both samples are two phases of mixed alcohols (phase 1) and hydrocarbons (phase 2), which are immiscible, at room temperature, as shown in inset of Fig. 5(a). Furthermore, the volume of phase 1 reaches 24-25% of the total volume of phase 1+phase 2 in all samples. In the 5 wt% Cu/AC catalyst, the liquid amount increases from 0.02 to 0.9 g/h as the GHSV increases from 6,000 h^{-1} to 18,000 h^{-1} at 30 bar and 300 °C. However, above GHSV 24,000 h^{-1}, the amount decreases to about 10%. In the case of 5 wt% Cu/TiO_2, the produced liquid corresponds more than 1.0 g/h, and increases with an increase of GHSV. The larger amount of liquid product in the 5 wt% Cu/AC than 5 wt% Cu/TiO_2 at the GHSV ranges of 6,000-18,000 h^{-1} can be caused by larger BET specific surface area of 5 wt% Cu/AC (~800 m^2/g) than 5 wt% Cu/TiO_2 (~8 m^2/g). However, a high GHSV (24,000 h^{-1}) in 5 wt% Cu/TiO_2 can increase the portion of heavy hydrocarbons (C_{10}-C_{15}) because of short residence time of gas phase and velocity fluctuations in catalyst bed of the reactor, as shown in Fig. 8. Fig. 5(b) shows the pressure effect

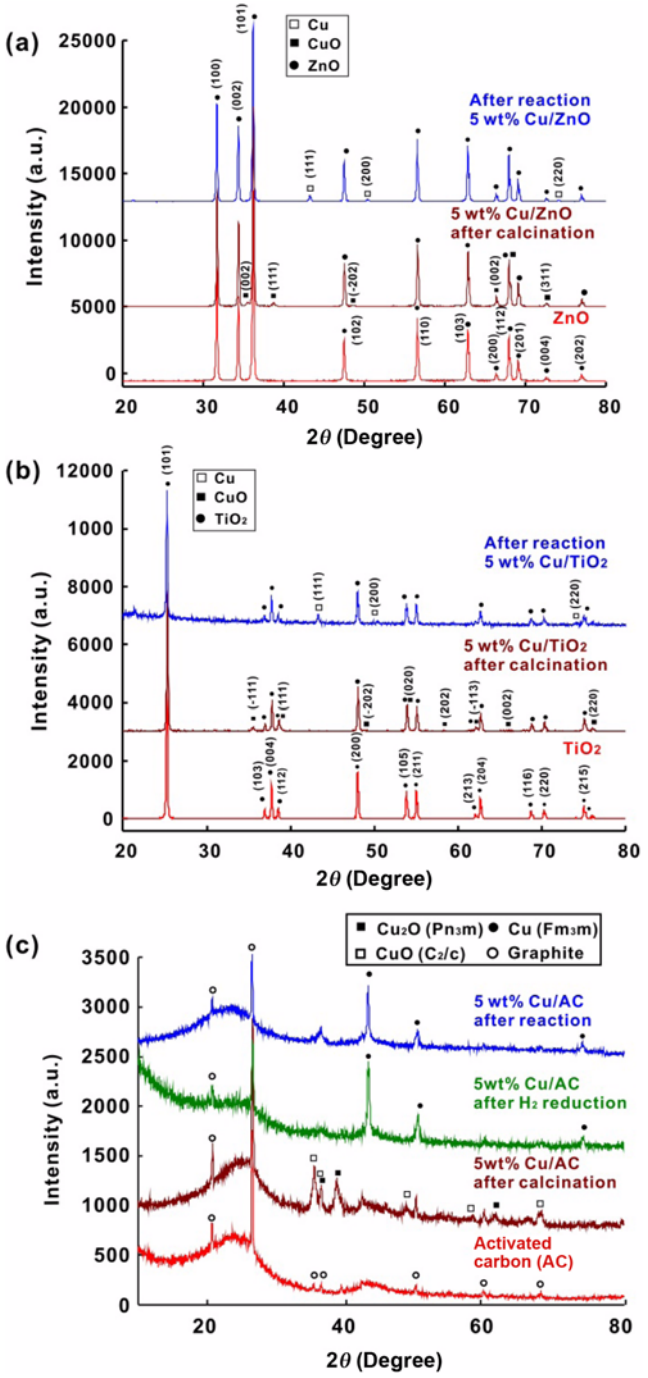

Fig. 4. X-ray diffraction (XRD) of 5 wt% Cu-based catalysts as support, ZnO (a), TiO_2 (b), AC (c) before and after H_2 reduction and catalytic reaction.

for liquid produced at 300 °C and 18,000 h^{-1}. In contrast with the result of 5 wt% Cu/ZnO, the liquid amount tends to increase with increasing pressure for both 5 wt% Cu/AC and 5 wt% Cu/TiO_2.

The liquid products were analyzed by GC-MASS spectroscopy and the peak identification for mass spectrometry data was carried out with the GC-MS Wiley database. Fig. 6 shows the GC-Mass spectra of phase 1 (a), phase 2 (b), and a small range (from 16 to 22 min) of phase 2 obtained from the 5 wt% Cu/AC catalyst. The spectra of these compounds matched those of the Wiley library well

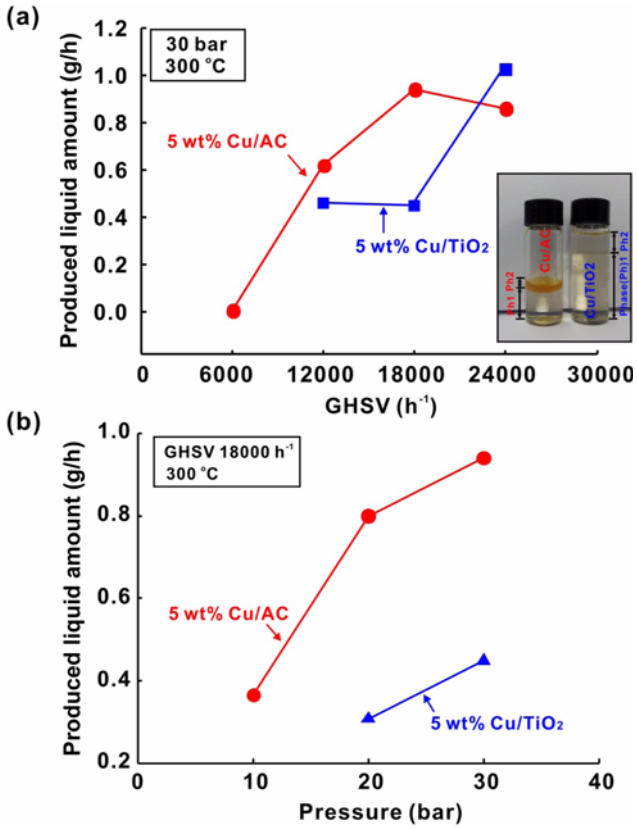

Fig. 5. The produced amount of liquid phase of 5 wt% Cu/AC and 5 wt% Cu/TiO_2 on the variance of (a) GHSV and (b) pressure of 5 wt% Cu/AC and 5 wt% Cu/TiO_2.

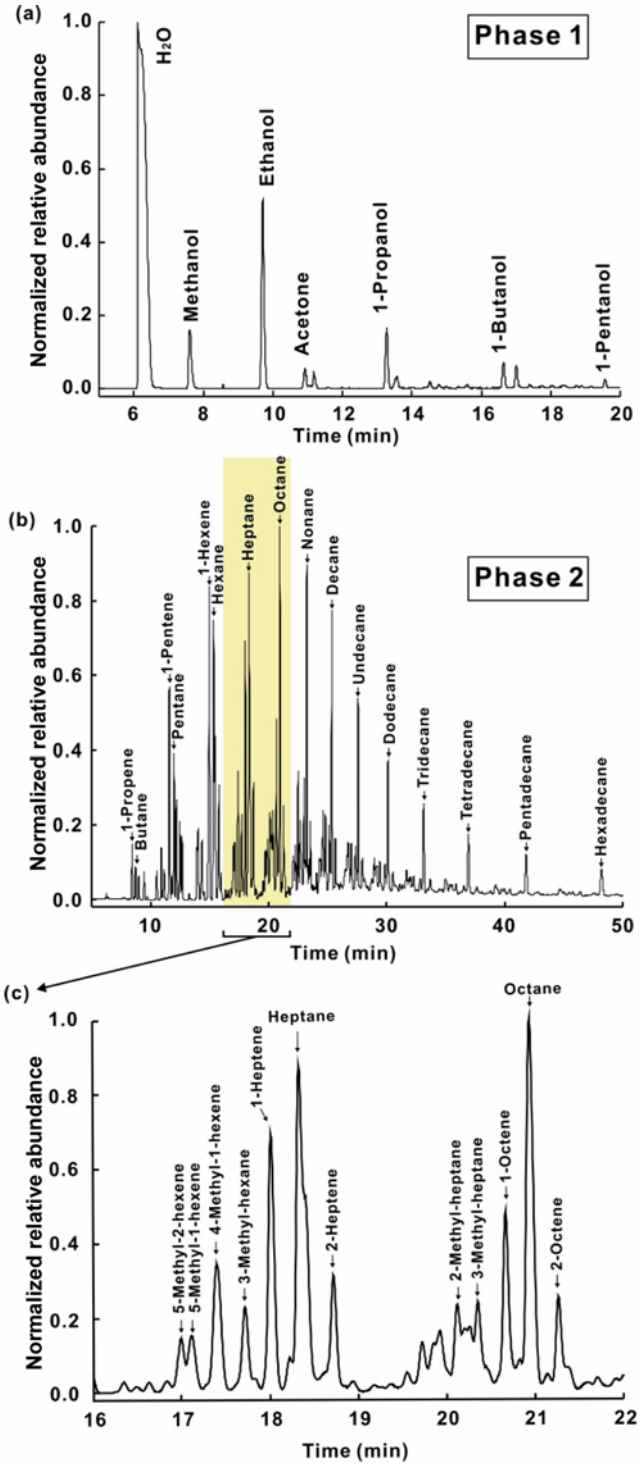

Fig. 6. GC-Mass spectra of phase 1 (a), phase 2 (b), and small range (16-22 min) of phase 2 obtained from 5 wt% Cu/AC.

and their structures were identified by % similarity values. The % similarity, molecular ion peaks, and base peaks are reported by Table S3. In phase 1, major peaks of the GC-MASS spectra revealed the presence of H_2O, methanol, and higher alcohols. It is seen that the amount of ethanol is larger than other alcohols, except for the H_2O amount. In the produced hydrocarbons of phase 2, typical stretching frequencies of saturated (alkane) hydrocarbons are observed, and the main peaks detected here are from hexane to hexadecane. To analyze the time-dependent change of the liquid component, we collected the produced liquid every 5 hours and analyzed it (Fig. 7). While phase 1 was little changed, phase 2 indicated that C4-C6 hydrocarbon disappear with increasing time. Fig. 8 shows the GC-Mass spectra of phase 1 (a), phase 2 (b), and a small range (from 16 to 22 min) of phase 2 obtained from the 5 wt% Cu/TiO_2 catalyst. Also, the % similarity, molecular ion peaks, and base peaks are reported by Table S4. The product from this catalyst shows a similar trend to the results obtained from the 5 wt% Cu/AC catalyst. Phase 1 and phase 2 indicate mixed alcohol products (H_2O, methanol, and higher alcohols) and hydrocarbons, respectively. However, the difference with previous 5 wt% Cu/AC sample is that the detected main peaks are simple alkene chains from 1-propene to 1-heptadecene (Fig. 6(b) and 6(c)). In comparing the components obtained from the three catalysts, Cu/ZnO, Cu/AC, and Cu/TiO_2, while Cu metal may participate in the production of both mixed alcohol and hydrocarbon, the supports, such as ZnO, AC, and TiO_2, influence the production of different types of hydrocarbon. However, the influences of the metal and support upon components of the product should be thoroughly more studied, because a strong metal-support interaction may be the key factor governing activity of the catalysts.

CONCLUSIONS

We studied the effects of different supports (ZnO, activated car-

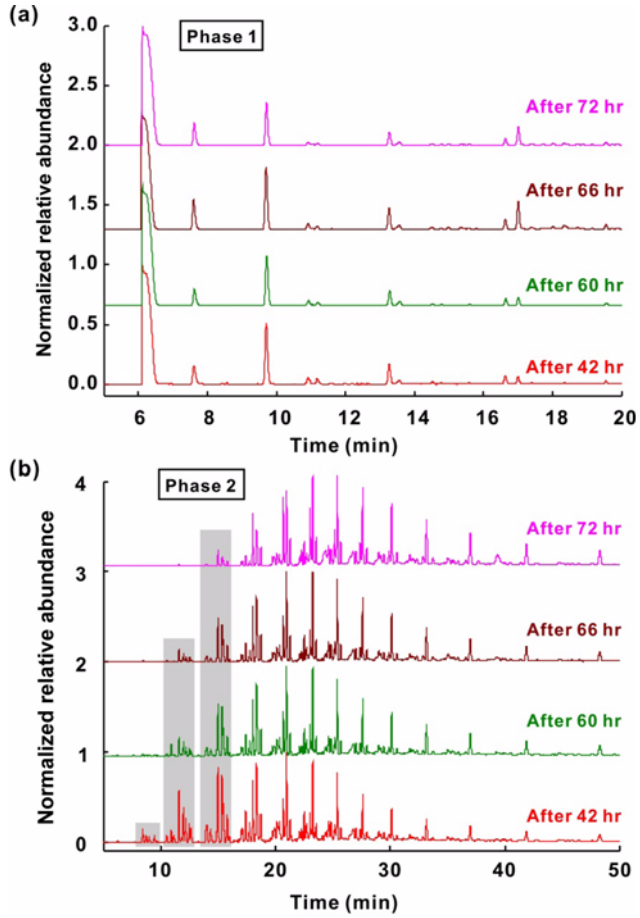

Fig. 7. GC-Mass chromatogram of phase 1 (a) and phase 2 (b) obtained from 5 wt% Cu/AC at different temperatures.

bon, and TiO_2) of Cu-based catalysts on alcohol-hydrocarbon synthesis from synthesis gas. While 5 wt% Cu/ZnO produced a single liquid phase of mixed alcohols, 5 wt% Cu/AC and Cu/TiO_2 created two phases, mixed alcohol (75%) and hydrocarbon (25%). At GHSV 18,000 h^{-1}, the amount of produced liquid of 5 wt% Cu/AC shows the highest value, 0.9 g/h. However, the amount of 5 wt% Cu/TiO_2 displays a sharp increase at GHSV 24,000 h^{-1}, which corresponds to 1.1 g/h. X-ray diffraction shows that CuO impregnated in the supports undergoes a complete reduction of metallic copper Cu^0, which is the real active phase in the catalytic process. All products obtained from the three catalysts include a mixed alcohol phase and hydrocarbon phase. However, in the Cu/ZnO catalysts, little hydrocarbon phase is produced. The Cu/TiO_2 catalyst showed highest ethanol composition in the mixed alcohol phase. Regardless of the support that is used, the produced liquids from Cu-based catalysts are separated by two phases, alcohol and hydrocarbon. However, the amount of produced liquid and compositions is dependent on the characteristics of the different supports. In the hydrocarbon phase of Cu/AC and Cu/TiO_2, the main peaks correspond to saturated (alkane) hydrocarbons from hexane to hexadecane and alkene chains from 1-propene to 1-heptadecene, respectively. These differences among the three catalysts may cause different interaction with Cu-support, but more study on the influences of the metal and support upon the components of the product is needed.

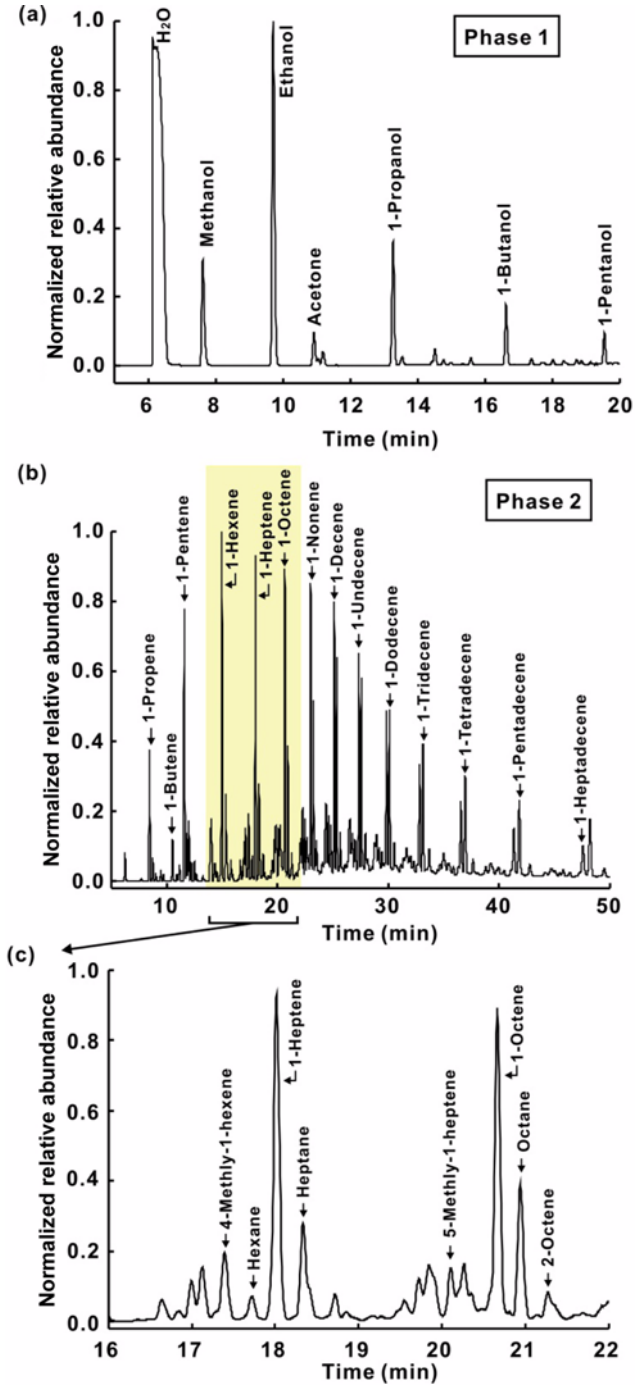

Fig. 8. GC-Mass spectra of phase 1 (a), phase 2 (b), and small range (16-22 min) of phase 2 obtained from 5 wt% Cu/TiO_2.

ACKNOWLEDGEMENT

This work was supported by the Korea Institute of Energy Research (KIER) grant funded by the Ministry of Knowledge Economy (MKE).

SUPPORTING INFORMATION

Additional information as noted in the text. This information is available via the Internet at http://www.springer.com/chemistry/jour-

nal/11814.

REFERENCES

1. J. C. Serrano-Ruiz and J. A. Dumesic, *Energy Environ. Sci.*, **4**, 83 (2011).
2. J. R. Rostrup-Nielsen, *Science*, **308**, 1421 (2005).
3. L. D. Schmidt and P. J. Dauenhauer, *Nature*, **447**, 914 (2007).
4. J. J. Spivey and A. Egbebi, *Chem. Soc. Reviews*, **36**, 1514 (2007).
5. V. Subramani and S. K. Gangwal, *Energy Fuels*, **22**, 814 (2008).
6. D. Mei, R. Rousseau, S. M. Kathmann, V.-A. Glezakou, M. H. Engelhard, W. Jiang, C. Wang, M. A. Gerber, J. F. White and D. J. Stevens, *J. Catal.*, **271**, 325 (2010).
7. M. M. Bhasin, W. J. Bartley, P. C. Ellgen and T. P. Wilson, *J. Catal.*, **54**, 120 (1978).
8. R. Burch and M. I. Petch, *Appl. Catal. A: Gen.*, **88**, 39 (1992).
9. R. Burch and M. I. Fetch, *Appl. Catal. A: Gen.*, **88**, 77 (1992).
10. M. Bhasin, *Catal. Lett.*, **59**, 1 (1999).
11. Z. Fan, W. Chen, X. Pan and X. Bao, *Catal. Today*, **147**, 86 (2009).
12. J. S. James and E. Adefemi, *Chem. Soc. Reviews*, **36**, 1514 (2007).
13. R. K. James, W. S. Arthur, G. Patricio, B. M. John, F. G. Edward and M. Scott, *Faraday Discuss Chem. Soc. Jpn.*, **72**, 121 (1981).
14. K. J. Smith and R. B. Anderson, *Can. J. Chem. Eng.*, **61**, 40 (1983).
15. D. J. Elliott and F. Pennella, *J. Catal.*, **114**, 90 (1988).
16. P. S. Gabor, T. Andras, H. Karoly and L. M. Jozsef, *Comb. Chem. High Throughpur. Screen*, **15**, 105 (2012).
17. C. T. Campbell, in: H. P. D. D. Eley, B. W. Paul (Eds.), Advances in Catalysis, Academic Press, 1 (1989).
18. B. A. Peppley, J. C. Amphlett, L. M. Kearns and R. F. Mann, *Appl. Catal. A: Gen.*, **179**, 31 (1999).
19. J. Nakamura, J. M. Campbell and C. T. Campbell, *J. Chem. Soc., Faraday Trans.*, **86**, 2725 (1990).

Supporting Information

Effect of support for alcohol-hydrocarbon synthesis from syngas in Cu-based catalyst

Sun-Hwa Yeon†, Dae-Hyun Shin, Nam-Sun Nho, Kyoung-Hee Shin, Chang-Soo Jin, and Sung-Chan Nam

Energy Storage Group, Korea Institute of Energy Research, 152, Gajeong-ro, Yuseong-gu, Daejeon 305-343, Korea
(*Received 21 June 2012 • accepted 26 November 2012*)

Table S1. The composition of produced mixed alcohol on 5 wt% Cu/ZnO at 300 °C, 30 bar, and GHSV 6,000 h^{-1}

Component	Retention time	Compositions (%)	
		5 wt% Cu/ZnO	3 wt% Cu/ZnO
H_2O	6.14	57.5	55.8
Methanol	7.61	5.0	7.3
Ethanol	9.72	15.3	18.2
Propanol	13.27	5.7	6.4
Butanol	16.66	2.7	3.3
Pentanol	19.56	1.2	1.4
Others		12.6	7.6

Table S2. Porosity characteristics of 5 wt% Cu supported on ZnO, AC, and TiO_2

Sample	Total pore volume (cm^3/g)	Mesopore volume (BJH-plot), (cm^3/g)	Micropore volume (t-plot)), (cm^3/g)
ZnO	0.026	0.024	-
AC	0.528	0.21	0.33
TiO_2	0.015	0.015	-
5 wt% Cu/ZnO	0.011	0.01	-
5 wt% Cu/AC	0.53	0.29	0.23
5 wt% Cu/TiO_2	0.033	0.031	-

Table S3. Retention time, % similarity, molecular ion peak, and base peak of 2 phases detected by GC-MS over 5 wt% Cu/AC

	Name of compound	Retention time (min)	% Similarity	Molecular ion peak (m/z)	Base peak (m/z)
Phase 1	Ethanol	9.750	91%	45.1	31.1
	Acetone	10.894	80%	58.1	43.1
	1-Propanol	13.305	94%	59.1	31.1
	1-Butanol	16.622	56%	74.1	56.1
	1-Pentanol	19.539	80%	70.1	42.1
Phase 2	Butane	8.724	83%	58.1	43.1
	Pentane	12.002	91%	72.1	43.1
	Hexane	15.327	87%	86	57.1
	Heptane	18.357	81%	100.2	43.1
	Octane	20.924	72%	114.2	43.1
	Nonane	23.213	91%	128.2	43.1
	Decane	25.346	96%	140.2	57.1
	Undecane	27.519	91%	154.2	57.1
	Dodecane	30.085	96%	170.2	57.1
	Tridecane	33.124	97%	207.1	57.1
	Tetradecane	36.919	97%	281.1	57.1
	Pentadecane	41.852	97%	281.1	57.1
	Hexadecane	48.246	97%	281.1	57.1

Table S4. Retention time, % similarity, molecular ion peak, and base peak of 2 phases detected by GC-MS over 5 wt% Cu/TiO_2

	Name of compound	Retention time (min)	% Similarity	Molecular ion peak (m/z)	Base peak (m/z)
Phase 1	Ethanol	9.646	91%	45.1	31.1
	Acetone	10.911	86%	58.1	43.1
	1-Propanol	13.244	91%	59.1	31.1
	1-Butanol	16.638	72%	74.1	56.1
	1-Pentanol	19.522	90%	79.1	42.1
Phase 2	1-propene	8.477	93%	41.1	56.1
	1-butene	10.516	91%	70.1	55.1
	1-pentene	11.582	91%	70.1	55.1
	1-Hexene	15.021	94%	84.1	56.1
	1-Heptne	18.060	96%	98.2	56.1
	1-Octene	20.705	95%	112.2	55.1
	1-Nonene	22.999	98%	126.2	56.1
	1-Decene	25.132	98%	140.2	55.1
	1-Undecene	27.344	97%	154.2	55.1
	1-Dodecene	29.832	97%	160	55.1
	1-Tridecene	32.871	99%	207	55.1
	1-Tetradecene	36.505	99%	207	55.1